J Mater Sci: Mater Electron (2015) 26:1799–1805
DOI 10.1007/s10854-014-2613-8

Physical, magnetic and mechanical properties of Bi-2212 superconductors prepared by high pelletization pressure

M. Ersin Aytekin · Berdan Özkurt · İlker Sugözü

Received: 12 November 2014 / Accepted: 11 December 2014 / Published online: 17 December 2014

Abstract In this work, ceramic superconductors with nominal composition $Bi_{1.8}Sr_2Ca_{1.1}Cu_{2.1}O_y$ were produced by different pelletization pressures at high values varied from 1.5 GPa to 6 GPa. The effects of high pelletization pressure on the structural and magnetic properties of samples fabricated in this work were investigated by means of X-ray powder diffraction, scanning electron microscopy, dc electrical resistivity, magnetic hysteresis loop measurements and Vickers microhardness measurements. The room temperature resistivity of the samples significantly decreases when pelletization pressure is increased. M-H measurements were performed at T = 10 K and 25 K, respectively. In order to examine the J_C characterization of samples, Bean's critical model was used. It was found that sample D including pelletization pressures of 6 GPa have higher values of magnetization in all applied magnetic fields, indicating good connectivity between grains. Additionally, mechanical properties of samples are also characterized by microhardness measurements at room temperatures, indicating that microhardness values as well as J_c values in sample D enhanced due to its stronger couplings between grains compared to other samples.

M. Ersin Aytekin · B. Özkurt (✉)
Advanced Technology Research and Application Center, Mersin University, Yenisehir TR-33343 Mersin, Turkey
e-mail: berdanozkurt@mersin.edu.tr

B. Özkurt
Department of Energy Systems Engineering, Faculty of Tarsus Technology, University of Mersin, Mersin, Turkey

İ. Sugözü
Department of Automotive Engineering, Faculty of Tarsus Technology, University of Mersin, Mersin, Turkey

1 Introduction

Bi-based superconductors among type II superconductors still have important advantages such as high chemical stability, relatively easy to obtain the formation of desired phases, enhancements in their flux pinning capability by introducing strong flux pinning centers. Many works showed that the superconducting and magnetic properties of BSCCO ceramics can be improved by substitution or addition of metallic elements such as Na, Ni, Nb, B, Cd, Sn, Ag, Pb [1–14].

On the other hand, there are many useful methods to improve the superconducting properties of BSCCO system such as the sintering process and Laser Floating Zone (LFZ) technique ensuring more bulk structure with high aligned grains [15–18]. Nevertheless, basic properties of the BSCCO ceramics must be improved to make long length conductors with higher J_c and H_c capacities in the fabrication technology of the superconducting cables and wires.

Non-superconducting phases and crystallographic defects in BSCCO system can generally impair more uniform grain structure and better current flow. But, they also are necessary for effective pinning centers. Also, one of the effective methods to reach high J_c values is to dope alkaline elements such as Li, Na into the BSCCO system [14, 19, 20], ensuring phase formation in lower temperatures than the crystallization temperature of BSCCO ceramics sintered between 840 and 860 °C generally. If origin nucleations begin to crystallize in lower temperatures than from the their normal crystallization temperatures, the grain sizes can increase up to higher dimensions, which are necessary for more granular structure ensuring the desired large critical current density.

Another important factor for high J_c can be the applied pelletization pressure when prepared BSCCO ceramics.

Marconi et al. [21] have investigated the influence of pelletization pressure at applied moderate pressure values for Bi-2223 samples. That work indicated that the increase of pelletization pressure reduces porosity and leads to the improvement of contacts between the grains, causing the flow of electric currents in very low resistance values.

In this work, the influence of pelletization pressures applied at high values on superconducting properties of $Bi_{1.8}Sr_2Ca_{1.1}Cu_{2.1}O_y$ ceramics prepared by the conventional solid-state reaction method was investigated by using X-ray powder diffraction (XRD), SEM, electrical resistivity, magnetic and mechanical measurements.

2 Experimental details

High purity powders of commercial Bi_2O_3 (Panreac,98+ %), $SrCO_3$ (Panreac, 98+ %), $CaCO_3$ (Panreac, 98.5+ %), CuO (Panreac, 97+ %) were used for the preparation of samples in this work. Polycristalline samples with nominal composition $Bi_{1.8}Sr_2Ca_{1.1}Cu_{2.1}O_y$ were prepared by the standard solid-state reaction methods. Firstly, they were weighed in the appropriate proportions, mixed and milled. After milling process, the homogenous mixture of powders was pressed into pellets of 2.9 cm diameter by applying different pelletization pressures using (1.5, 3, 4.5, and 6 GPa) at room temperature and then calcined at 750 °C for 12 h. After the calcined pellets were reground thoroughly, they were repressed within different pressure values applied as uniaxial at room temperature and re-calcined at 820 °C for 24 h to start the formation of the superconducting phase. These processes based on the milling, sintering and pressing were repeated two times. Finally, precursor materials including different pelletization pressures were annealed at 850 °C for 120 h in air to produce the Bi-2212.

Taking into account the pelletization pressure values, the samples will be herein after denoted as A, B, C and D, respectively.

Resistivity and magnetic measurements were carried out on samples using Cryogenic Limited PPMS (from 5 to 300 K) which can reach the cryogenic temperatures about to 2 K in a closed-loop He system. X-ray powder diffraction analyses to determine the phases present in the samples were performed by using a Rigaku Ultima IV X-ray diffractometer with a constant scan rate (2°/min) in the range $2\theta = 3$–60°. The surface morphologies of the samples were studied by using a Zeiss/Supra 55 Scanning Electron Microscopy (SEM).

The Vickers microhardness measurements of samples were performed in a Micro Hardness Tester (Model HV-1000) at room temperature. A Vickers indenter with different loads (0.245, 0.49, 0.981, 1.962, 2.943, 4.905, and 9.81 N) and a loading time of 20 s was used. An average of 20 readings of the diagonals of the indentation, at different locations on the surface of the samples, for each load was taken to obtain the most accurate values of microhardness.

The pressing of samples was made by using Special Press with model version 22170, which can reach the maximum pressures about to 15 GPa pressing force with 1,300 × 1,600 mm table sizes designed by Hursan Hydraulic Press and Workbech Ind.Set.CO, ODCP Series.

Also, hardened to 48HRC steel mold was used in order to press the samples at targeted pressing forces.

3 Results and discussion

3.1 XRD studies

First, we deal with the phase composition of the samples produced by using high pelletization pressure. XRD patterns for all samples are shown in Fig. 1. While dominant phase is Bi-2212 in all samples, there are also some impurity phases such as $Bi_{0.75}Sr_{1.25}O_3$ and Bi_2CaO_4 (shown in Fig. 1 by * and, respectively). The automatically obtained lattice parameters a, b, and c is listed in Table 1. While sample A has orthorhombic crystal symmetry, other samples including higher pelletization pressure have tetragonal structure, which is the proof of that pelletization pressure plays an important role on anisotropy of samples. The characteristic peaks of Bi-2212 phase in all samples appear at points such as $2\theta \approx 5.7°$; 24.8°; 29.1° and etc. Also, the width and intensity of these peaks in all samples

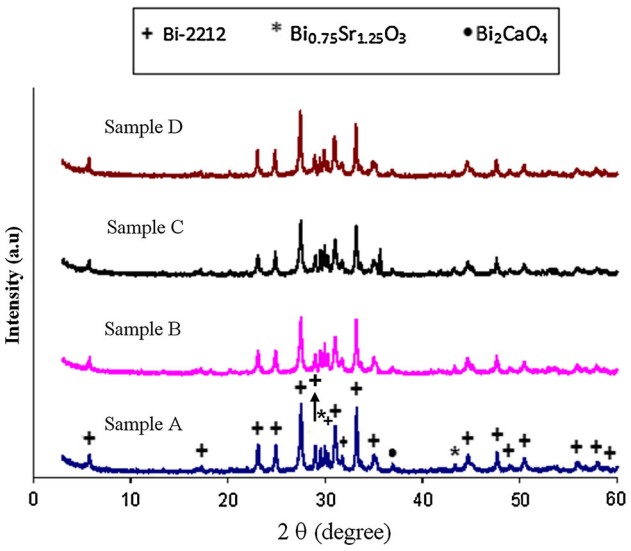

Fig. 1 XRD patterns of the *A*, *B*, *C*, and *D* samples. Bi-2212 diffraction peaks are identified by *plus*. The peaks of $Bi_{0.75}Sr_{1.25}O_3$ and Bi_2CaO_4 are shown by *asterisk* and *dot*, respectively

Table 1 Crystal parameters and resistivity measurement results for the samples

Samples	a (Å)	b (Å)	c (Å)	T_c^{onset} (K)	T_c^{offset} (K)	R (mohm-cm) at 300 K	Hole conc. (p)
A	5.399	5.378	30.778	74.1	41.92	7.84	0.0816
B	3.816	3.816	30.799	68.3	47.8	3.1	0.0872
C	3.818	3.818	30.802	70.3	50.3	3.2	0.0896
D	3.819	3.819	30.880	72.3	57.3	2.23	0.0971

are almost same. This may be related to the fact that samples have similar phases although they can have different grain couplings and grain sizes by applying different pelletization pressures.

On the other hand, lattice parameters were determined from the XRD diffraction data as a = 5.399 Å, b = 5.378 Å, c = 30.778 Å; a = b = 3.816 Å, c = 30.799 Å; a = b = 3.818 Å, c = 30.802 Å; and a = b = 3.819 Å, c = 30.880 Å for the samples A, B, C and D, respectively.

It is clear that lattice parameter c increases gradually with increasing pelletization pressure, indicating that interatomic distance in Bi–O planes increases as depending on the changing amount of oxygen possibly. It is well known that there is the oxygen deficiency in Bi–O planes although pure Bi-2212 ceramics have enough excess amount of oxygen [22, 23]. Bi–O planes to achieve energetically more stable structure can generally prefer to capture the oxygen, causing a regular contraction in the c-axis due to the increasing of positive charges in Bi–O planes. However, the length of the c-axis in all samples produced by high pelletization pressures in this work systematically increases, implying that Bi–O planes prefer to release their poor oxygen rather than to capture the oxygen.

3.2 SEM analyses

Figure 2 shows the characteristic SEM pictures of the all samples. The microstructures of all samples shows that there are many plate-like and flaky shaped grains together with some voids and secondary phases between grains, meaning that the Bi-2212 phase in all samples is mainly formed. However, sample D produced at 6 GPa shows more dense and granular structure due to the agglomeration and enlargement of grains which causes to the decreasing of voids. When Bi-2212 ceramics are prepared by the solid-state reaction method, it is possible lower crystallinity and more irregular grain arrangements rather than texture structure because of their high anisotropic characteristic. Generally, the selected time and temperature values in the annealing process of BSCCO ceramics plays an important role in their surface structures due to the changing shape, size and structure of grains.

Thus, it can be expected that all samples produced in this work can show the similar surface mobility, because of they are kept at the same temperature and time in the high-temperature furnace. However, it is clearly seen from the SEM figure that with increasing pelletization pressure voids and porosity started to decrease by the formation of bigger plate-like grains. Based on these results, high pelletization pressure leads to the more granular structure with improving grain sizes and decreasing voids. Note that although the surface morphology positively changes with increasing pelletization pressure, randomly distributed grains and different connectivity between intergrains can significantly change the superconducting properties of samples.

3.3 Electrical measurements

The temperature dependence of resistivity of all samples is given in Fig. 3. It is observed that the room temperature resistivity of samples significantly decreases with increasing pelletization pressure, indicating the improvements in the quality of contacts between grains. HTSs can show the sharpness in their transition from a normal state to superconducting phase if they only consist of a single type phase without including multi-phase and a large number of impurity phases. It can be seen from Fig. 3 all samples show similar transitions after their metallic behavior up to their T_c^{onset} temperatures even if their values are different, indicating that all samples have same phases, which confirm the XRD analysis. The T_c^{offset} is found to be 57.3 K fthe valuemplethe samplereas T_c^{offset} value of sample A is 41.92 K, indicating that the values of the applied pelletization pressure are rather sensitive to links between grains. According to the findings of the resistivity measurements, the pelletization pressure of 6 GPa is determined to be the best value for the less voids and better connectivity between grains.

3.4 Carrier concentration calculations

The hole-carrier concentrations per Cu ion, P, are calculated by means of the following relation [24]:

$$P = 0.16\left[\left(1 - \frac{T_C^{offset}}{T_C^{\max}}\right)/82.6\right]^{1/2}$$

where $T_C^{\max}$ is taken as 85 K for Bi-2212 phase [25, 26] and T_C^{offset} values are those shown in Table 1. Figure 4 indicates the variations of hole-carrier concentrations as a function of

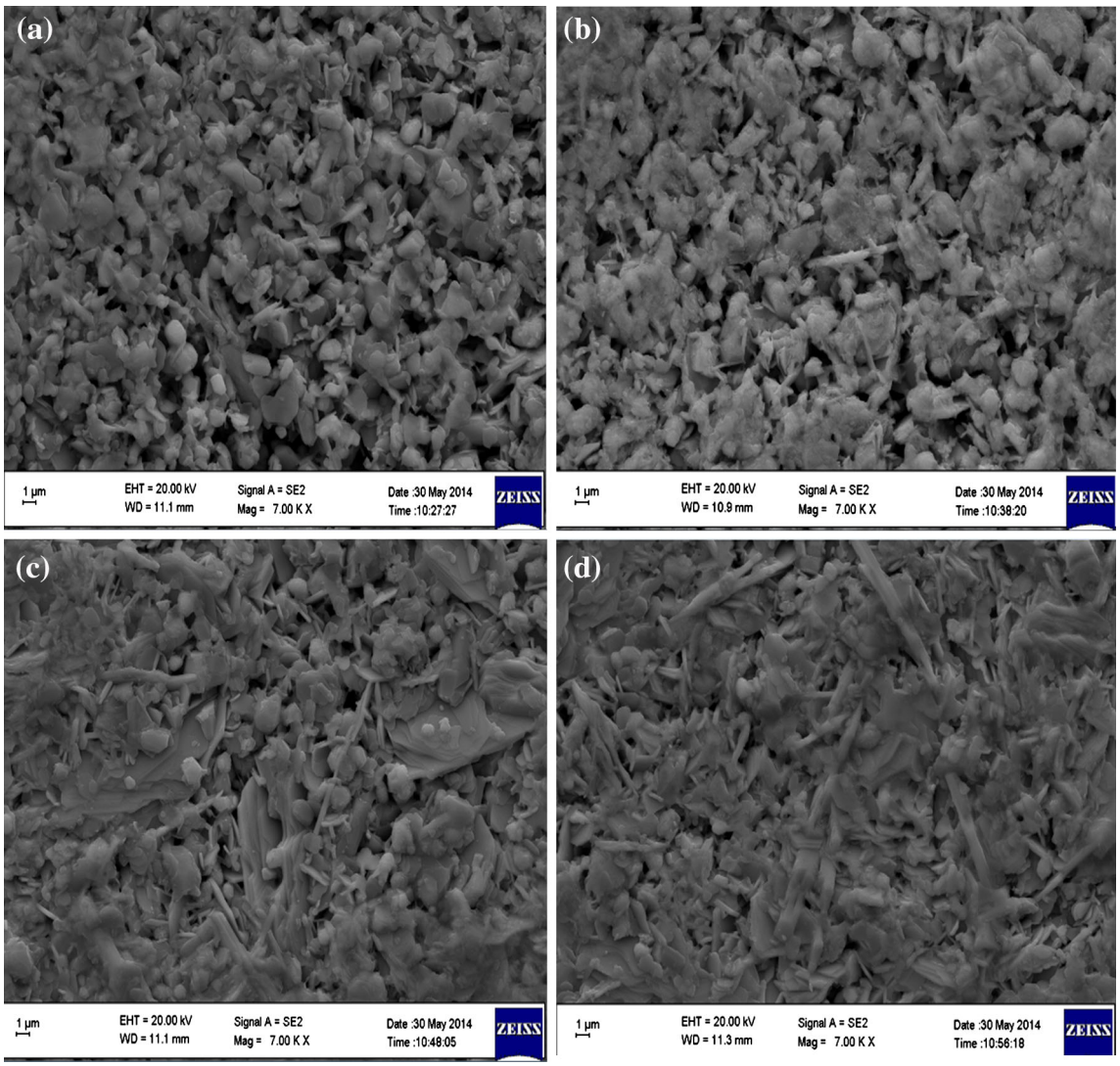

Fig. 2 SEM micrographs obtained in the surfaces of **a** A; **b** B; **c** C; and **d** D samples

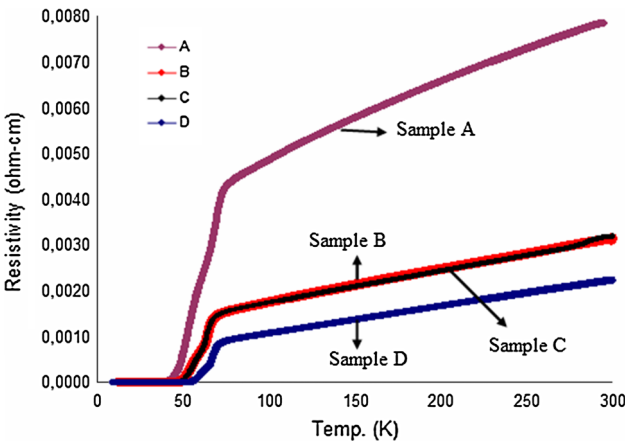

Fig. 3 Electrical resistivity as a function of temperature curves for all the samples

increasing pelletization pressure, showing the increase of hole-carrier concentration p with increasing pelletization pressure. It is well known that T_C^{onset} values strongly depend on the intra-grain features due to the degree of the transition within grains while T_C^{offset} values are closely connected with intergrain properties as based on powerful or weak coupling between grains. Hole carrier concentration increases from 0.0816 for sample A to 0.0971 for sample D. Thus, the increasing hole concentration with increasing pelletization pressure is an important evidence for improving grain connectivity.

3.5 Magnetic properties

The magnetic-hysteresis cycles, between applied fields of ±2 T, for all the samples at 10 and 25 K, are presented in

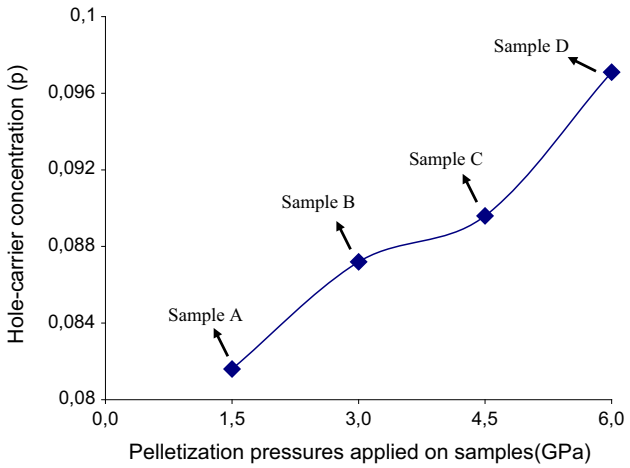

Fig. 4 Variation of hole-carrier concentration versus pelletization pressures applied on samples

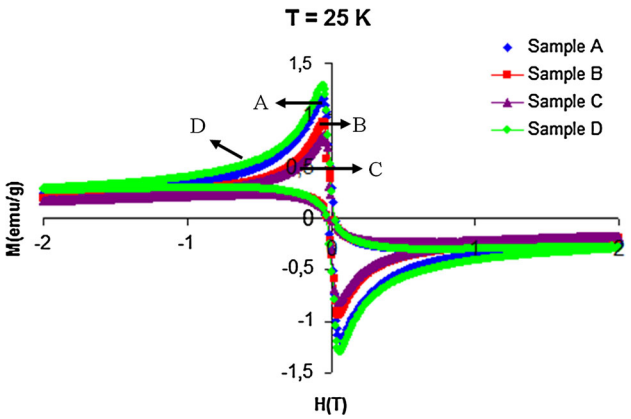

Fig. 6 Magnetization hysteresis curves for all samples measured at 25 K and ±2 T external applied magnetic field

Figs. 5 and 6, respectively. It is well known that M-H loops of HTSs can also be used for determining the presence of flux-pinning centers. It can be seen from both Figs. 5 and 6. That the value of remnant magnetization (M_R) for sample D is the highest, implying the increases in pinning strength which is directly proportional to M_R [27]. In addition, symmetrical behaviors in hysteresis loops of samples also can suggest the existence of such flux-pinning centers. The important enhancement of M_R value in sample D compared to other samples can also be explained by the decreases in intergranular pores, as seen from SEM micrographs in Fig. 2. On the other hand, the remarkable increase in the length of the c-axis lattice constant observed for sample D may also create appropriate spin orientation in the crystallographic unit cell of Bi-2212 due to a relaxation in the overlapping of nearest-neighbor orbital. In addition, the

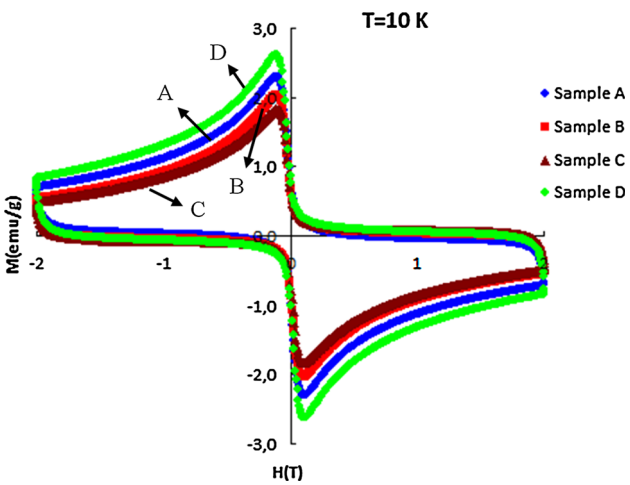

Fig. 5 Magnetization hysteresis curves for all samples measured at 10 K and ±2 T external applied magnetic field

magnetic hysteresis cycles of all samples performed at T = 25 K as seen in Fig. 6 also show that sample D still protects its the strongest diamagnetic behavior, although there are the decreases in its M_R values due to the weak pinning of flux at the relatively high temperature, indicating that it has a common vortex behavior of type II superconductors.

The J_C values of the samples were calculated at T = 10 K, using the Bean's model [28]:

$$J_c = 30\,\frac{\Delta M}{d}$$

where J_C is the magnetization current density in ampéres per square centimeter of a sample. $\Delta M = M_+ - M_-$ is measured in electromagnetic units per cubic centimeter, d is the diameter of cylindrical samples [13]. Figure 7 shows the effect of high pelletization pressure on intergrain critical current density (J_c) of the Bi-2212 ceramics. J_c for the sample D significantly improves while both sample B and C have less J_c value compared to sample A prepared with lowest pressure value in this work. Sample D exhibits a J_c of 82×10^4 A/cm^2 at H = 0.5 T while J_c is 34×10^4 A/cm^2 for sample C including the smallest J_c value obtained at T = 10 K in this work. Note that J_c calculated from Bean's model always shows higher values than the values obtained by transport critical current density determined from I–V curves.

Irregular orientation and size of grains, high anisotropy, weak links and voids between grains, impurity phases in the grain boundaries are the main factors determined the values of J_c in high-T_c superconductors, which strongly depend on the preparation techniques of materials. The high Jc value of sample D reveals that the optimal pelletization pressure of 6 GPa ensures improved intergranular contacts with less voids. Also, J_c values for all samples were calculated in the whole magnetic field range (0–2T), indicating that the above factors in the determining of Jc

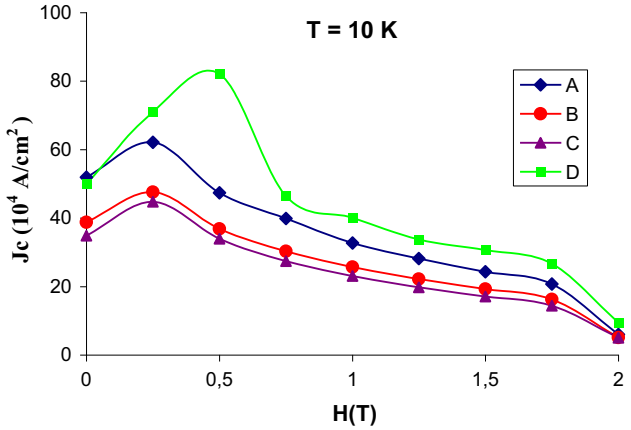

Fig. 7 Calculated critical current densities for all the samples at 10 K as a function of applied field

values at these low magnetic ranges are more effective rather than the contribution of effective pinning centers. Thus, it can be said that the enhancements in sample D strongly depend on intergrain effects.

3.6 Mechanical properties

Also, high microhardnes values in BSCCO ceramics are essential for their applications in technological areas. There is an important correlation between weak links in the grain boundaries and microhardness values in BSCCO ceramics. While high pelletization pressures can cause to improving in size and binding energy of grains, they also can create many impurity phases causing disruptions in the transmission of superconducting currents.

The microhardness graph shown in Fig. 8 for all samples is essential to better interpret the high pelletization pressure effect on BSCCO ceramics.

The Vickers microhardness values (H_V) for all samples were calculated using the traditional definition [29, 30];

$$H_V = 1854.4\left(\frac{P}{d^2}\right)(GPa),$$

where P is the applied load in N and d is the diagonal length of the indentation mark in μm.

As can be seen from this figure, the microhardness values systematically increased with increasing pelletization pressure. On the other hand, microhardness value of both sample A and D increases with the applied load after load of 2 N, while the microhardness of both sample B and C decreased with increasing load after applied 2 N load values.

Nonlinear behavior of microhardness up to 2 N load values for all samples is related with surface properties of samples, since such small loads applied can not approach to more inner structures including parameters such as grain alignments, voids, connectivity between grains. Further,

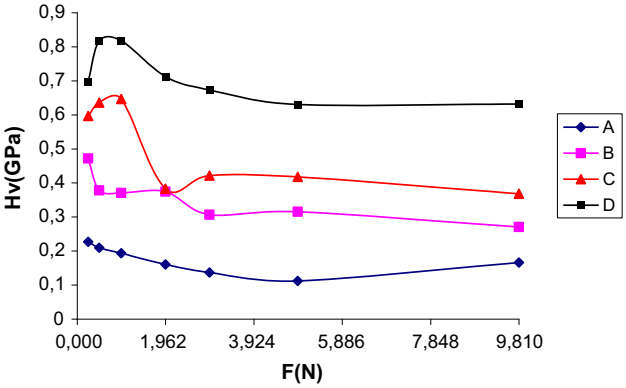

Fig. 8 Microhardness evolution with the applied load for the different samples

the microhardness values are attained to increase to 0.165 and 0.631 GPa for the A and D samples, respectively. These results indicate that the coupling and connectivity between superconducting grains in sample D significantly enhance.

4 Conclusions

In summary, the effect of high pelletization pressure applied during the preparing of the Bi-2212 ceramics on structure, magnetic and mechanical properties has been investigated. The hole carrier concentration increases from 0.0816 to 0.0971 with increasing pelletization pressure. The sample D has the lowest room temperature resistivity amongst the samples, showing that it has the optimum number of holes induced in the oxygen sites of the CuO_2 layers.

The microhardness value of the sample D including the greatest pelletization pressure is observed to be higher than other samples.

Acknowledgments This work is supported by the BAP Research Fund of Mersin University, Mersin, Turkey, under Grant Contracts No: BAP-FBE ESMB (MEA) 2014-3 YL and BAP-TTEF MEOEB (İS) 2012-8 A. All samples have been prepared in the MEİTAM Central Laboratory in Mersin University in Turkey. Both SEM and XRD measurements have been made in the MEİTAM Central Laboratory in Mersin University, the other measurements in this study have been made in the METU Central Laboratory in Middle East Technical University in Ankara in Turkey. On the other hand, I wish to thank M.Sc. Aynur GURBÜZ and PhD. M. Serkan YALÇIN in the MEİTAM Central Laboratory and Dr. Ibrahim ÇAM in the METU Central Laboratory for their experimental support and very meticulous work.

References

1. H. Sözeri, N. Ghazanfari, H. Özkan, A. Kılıç, Supercond. Sci. Technol. **20**, 522 (2007)

2. A. Sotelo, M. Mora, M.A. Madre, J.C. Diez, L.A. Angurel, G.F. de la Fuente, J. Eur. Ceram. Soc. **25**, 2947 (2005)
3. L. Jiang, Y. Sun, X. Wan, K. Wang, G. Xu, X. Chen, K. Ruan, J. Du, Phys. C **300**, 61 (1998)
4. M. Zargar Shoushtari, S.E. Mousavi Ghahfarokhi, J. Supercond. Nov. Magn. **24**, 1505 (2011)
5. A.I. Abou-Aly, M.M.H. Abdel Gawad, R. Awad, I. G-Eldeen, J. Supercond. Nov. Magn. **24**, 2077 (2011)
6. M. Mora, A. Sotelo, H. Amaveda, M.A. Madre, J.C. Diez, L.A. Angurel, G.F. de la Fuente, Bol. Soc. Esp. Ceram. **44**, 199 (2005)
7. S. Şakiroğlu, K. Kocabaş, J. Supercond. Nov. Magn. **24**, 1321 (2011)
8. S.M. Khalil, J. Phys. Chem. Solids **62**, 457 (2001)
9. A. Sotelo, M.A. Madre, J.C. Diez, Sh Rasekh, L.A. Angurel, E. Martinez, Supercond. Sci. Technol. **22**, 034012 (2009)
10. M.A. Madre, H. Amaveda, M. Mora, A. Sotelo, L.A. Angurel, J.C. Diez, Bol. Soc. Esp. Ceram. **47**, 148 (2008)
11. Y.L. Chen, R. Stevens, J. Am. Ceram. Soc. **75**, 1150 (1992)
12. R. Ramesh, S. Green, C. Jiang, Y. Mei, M. Rudee, H. Luo, G. Thomas, Phys. Rev. B: Condens. Matter **38**, 7070 (1988)
13. B. Ozkurt, J. Alloy. Compd. **579**, 132 (2013)
14. B. Ozkurt, J. Mater. Sci. **24**, 2426 (2013)
15. B. Özçelik, B. Özkurt, M.E. Yakıncı, A. Sotelo, M.A. Madre, J. Supercond. Novel Magn. **26**, 873 (2013)
16. B. Özkurt, M.A. Madre, A. Sotelo, M.E. Yakıncı, B. Özçelik, J. Supercond. Novel Magn. **25**, 799 (2012)
17. B. Özkurt, M.A. Madre, A. Sotelo, M.E. Yakıncı, B. Özçelik, J.C. Diez, J. Supercond. Novel Magn. **26**, 1093 (2013)
18. B. Ozkurt, M.A. Madre, A. Sotelo, J.C. Diez, Phys. B **426**, 85 (2013)
19. B. Ozkurt, J. Mater. Sci.: Mater. Electron. **25**, 3295 (2014)
20. O. Bilgili, Y. Selamet, K. Kocabas, J. Supercond. Nov. Magn. **21**, 439 (2008)
21. D. Marconi, C. Lung, A.V. Pop, J. Alloys Comp. **579**, 355 (2013)
22. S. Satyavathi, M. Muralıdhar, K. Nandakishore, V. Hari Babu, O. Pena, M. Sergent, F. Beniere, Appl. Supercond. **3**, 187 (1995)
23. V.P.S. Awana, S.K. Agarwal, R. Ray, S. Gupta, A.V. Narlikar, Phys. C **191**, 43 (1992)
24. B.F. Azzouz, A. Mchirgui, B. Yangui, C. Boulesteix, B.M. Salem, Phys. C **356**, 83 (2001)
25. T. Kucukomeroglu, E. Bacaksız, C. Terzioglu, A. Varilci, Thin Solid Films **516**, 2913 (2008)
26. S. Bal, M. Dogruer, G. Yildirim, A. Varilci, C. Terzioglu, Y. Zalaoglu, J. Supercond. Nov. Magn. **25**, 847 (2012)
27. B.A. Albiss, I.M. Obaidat, M. Gharaibeh, H. Ghamlouche, S.M. Obeidat, Solid State Commun. **150**, 1542 (2010)
28. C.P. Bean, Phys. Rev. Lett. **8**, 250 (1962)
29. A. Leenders, M. Ullrich, H.C. Freyhardt, Phys. C **279**, 173 (1997)
30. M. Yilmazlar, O. Ozturk, H. Aydın, M. Akdoğan, C. Terzioğlu, Chin. J. Phys. **45**, 128 (2007)